Spectroscopic and Computational Studies of Gas Phase Hydrogen Bound Clusters of 9-Hydroxy-9H-Fluorene-9-Carboxylic Acid

by

Thomas Kuntz
Class of 2012

A thesis submitted to the
faculty of Wesleyan University
in partial fulfillment of the requirements for the
Degree of Bachelor of Arts
with Departmental Honors in Chemistry

Abstract

A longstanding goal of chemists has been to deeply analyze fundamental molecular parameters, such as vibrational frequencies and electronic properties, and basic chemical interactions, such as hydrogen bonding, in order to better understand increasingly complex molecules and molecular clusters. A mixture of jet-cooled laser spectroscopic techniques and *ab initio* quantum chemical calculations is applied for this purpose on the chromophore 9-hydroxy-9H-fluorene-9-carboxylic acid (9FCA) and its gas phase hydrogen bound clusters with various ligands. Discovery and exploration of systems exhibiting conformational flexibility is of particular interest. A somewhat novel multiple conformer system produced by variations in binding partner conformation rather than variations in chromophore conformation was observed spectroscopically; other similar systems were found computationally but without full experimental confirmation.

Acknowledgements

I'd like to thank my family, friends, advisor, lab-mates, house-mates, casual acquaintances, etc. I've run out of time to write this, but imagine I'm saying something nice about you. I would if I had time to. Really.

Table of Contents

Ch 1: Introduction

Jet-cooled laser spectroscopy has its beginnings in the work of Kantrowitz and Grey[1] who pioneered the jet-cooling process as a high intensity source for molecular beams. Groups such as Levy et al.[2, 3] quickly applied this molecular beam technique for spectroscopic ends because of its remarkable effect on molecular state distributions. Jet cooling has the incredible ability to generate ultra-cold (rotational temperatures of ~10 K) molecules in the gas phase through collisional interactions with an inert carrier gas, typically helium or argon. It also causes controlled partial condensation of molecular clusters[4], allowing for the exploration of their intermolecular interactions. This process is preferable to cooling with refrigerants when the goal is to investigate molecular parameters and interactions in fine detail; refrigerating molecules usually leads to their condensation, which introduces interactions and effects which obscure those at a smaller scale, giving rise to spectra with broad transitions. Jet-cooled gas phase spectra are conversely characterized by their resolution of individual molecular rotations and vibrations, because of the lack of these bulk effects and the high degree of cooling which is enough to bring most molecules to their ground states. Lasers, particularly tunable ones, are useful tools for spectroscopy under these conditions because they give off nearly monochromatic, intense light, allowing for precise excitation of well-defined molecular states from the ground state with high sensitivity and low background noise.

The work in this thesis utilizes ultraviolet and infrared pulsed dye lasers to apply a number of techniques of jet-cooled laser spectroscopy to a chromophore, a

molecule which absorbs strongly in the UV, and its hydrogen bound clusters. These techniques are Resonance Enhanced Multi-Photon Ionization (REMPI) and the related IR-UV double resonance, IR-UV hole-burning, and UV-UV hole-burning[5]. REMPI spectroscopy is used to produce electronic spectra and possesses the useful properties of yielding ions, which can be easily separated by mass, and of utilizing multi-photon processes, which can be used to observe different types of transitions than single photon processes, on account of differing selection rules[6]. IR-UV double resonance provides cold, sharp IR spectra through the depletion of a signal from a UV resonance. IR-UV hole-burning entails fixing the IR laser frequency to an IR peak of a molecule and scanning the REMPI spectrum to observe those molecules which do not resonate with the selected IR frequency. UV-UV hole-burning uses a high intensity burn laser fixed at a resonance of a molecular species to ionize and remove that species shortly before a second UV laser is introduced to perform a REMPI scan. This, when subtracted from a traditional REMPI scan taken concurrently, produces an electronic spectrum which only shows the targeted molecular species.

One focus of this research is the spectroscopic detection and separation of conformational isomer signals. Many molecules exist in multiple distinct forms separated by rotations around flexible bonds; these forms are called conformational isomers or conformers. Conformational isomers have the same mass as each other, since they consist of the same atoms with the same connectivity, so they can not be separated by standard mass spectroscopy. They often can be differentiated, however, by their differing IR spectra, and their electronic spectra can be made distinct by hole-burning techniques. This has been accomplished by a number of groups on single

molecules, such as acetaminophen[7], and a on number of molecular clusters including complexes of various chromophores with H_2O[8-10], argon[11], alcohols[12], and even alkaline earth metals[13].

Assignment of specific conformational geometries to their spectra signatures, rather than simply affirmation of the presence of multiple conformers, however, often requires more than just the described spectroscopic techniques. Detailed rotational and vibrational analyses are sometimes used, but these are often difficult and cannot always be performed. Thus, other methods must be found for this purpose.

Ab initio quantum chemical calculations provide one such tool. These calculations, rooted in the solution of the Schrödinger equation, give theoretical values for molecular parameters such as relative energies, vibrational frequencies, isomerization energies, and binding energies. These molecular parameters can obtained with strikingly high levels of accuracy for small molecules, even converging to the exact solution with enough computational power and time. For larger molecules like those studied here, a balance between accuracy and computational resources is vital, and often the best results possible only provide qualitative information. Nonetheless, this frequently leads to chemical insight difficult or impossible to obtain otherwise. For example, relative energy calculations can reveal which conformer is the dominant, minimum energy one and when coupled with a Boltzmann population analysis, can provide a gauge of the relative populations of lower energy conformers. Calculated vibrational frequencies can be compared those experimentally obtained, providing at best an absolute assignment of conformers or at minimum a basis for rejecting a certain calculated structure or calculational model.

Care needs to be taken when performing these types of analyses, however. Since measurements made *in silico* are almost always approximations of physical measurements, close attention needs to be paid to the specific approximations made and their effects, which vary from computational model to model. Occasionally, approximations give results which are misleading or not even qualitatively correct. Furthermore, when searching for the dominant structure of a system, it is impossible to know if the global energy minimum has actually been found without calculating the entire potential energy surface. Calculations generally optimize to local minima, unless transition states are targeted. While this is necessary for exploration of the higher energy conformational possibilities of a system, false identification of a structure as the global minimum will lead to faulty conclusions.

Our goal is to elucidate properties of hydrogen bound clusters with the chromophore 9-hydroxy-9H-fluorene-9-carboxylic acid (9FCA), with a concentration on conformational isomerism. We aim to recapitulate and expand on past work performed by Gu[14] in an attempt to address some of the questions left and to apply the previous techniques and insights to new molecular systems. 9FCA was chosen as a subject because it absorbs strongly in the UV region, giving a clear S_0-S_1 spectrum, and because it has hydroxyl groups that absorb at experimentally available IR wavelengths and are able to form hydrogen bound complexes.

In the past, Gu had looked at complexes with the carboxylic acids benzoic acid, acetic acid, and formic acid, as well as the analogously binding formamide. This investigation was briefly continued, utilizing additional binding partners of acrylic acid, propionic acid, and pyruvic acid. Complexes with diols were

subsequently examined because they present a system with more OH stretching vibrations than the carboxylic acid clusters. This was anticipated to produce richer activity in the IR spectra. Furthermore, the binding geometry is not clear on inspection, and multiple observable conformers seem possible; this makes diol complexes an interesting topic of study, both as an exploration of conformational flexibility, and as a general model for diol–carboxylic acid binding.

Ch 2: Experimental

2.1: Molecular Beam Apparatus

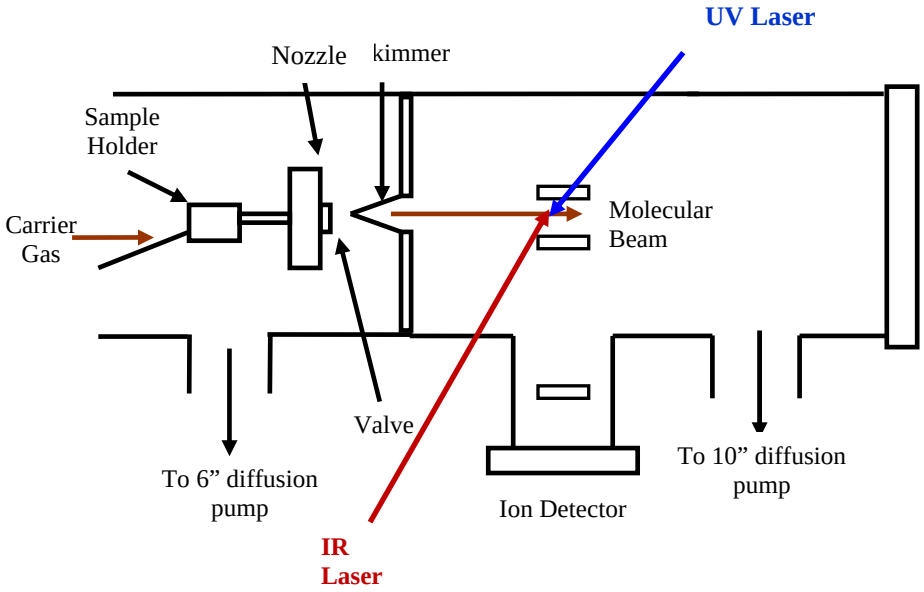

Figure 2.1.1: Arrangement of pulsed valve, nozzle, sample container, and skimmer inside two differentially pumped vacuum chambers.

Figure 2.1.1 gives a schematic of the molecular beam apparatus used in these experiments. It consists of two differentially pumped vacuum chambers separated by a conical skimmer with a diameter of 1 mm. The pressure in the first chamber is kept around 10^{-5} torr and the pressure in the second at 10^{-6} torr. To produce the molecular

beam, helium carrier gas is first flowed into the sample holder and nozzle and pulsed into the vacuum by a standard general valve (series 9) at a backing pressure of 15-20 psi and a pulse rate of 20 Hz. The conical skimmer collimates the supersonic jet into a beam as it passes through. The nozzle and chamber are each coupled to a heating element, which is necessary for sample preparation.

2.2: Time-of-Flight Mass Spectrometry

In all experiments performed, ions are ultimately produced, which can be separated by mass using time-of-flight techniques. This is because ions subjected to a simple electric field gain a velocity based on their charge to mass ratio. Given a fixed travel distance, these velocities result in a fixed flight time. Only singly charged positive ions are expected in the experiments performed, thus measured times-of-flight can be correlated to ionic masses.

In the current scheme, the lasers enter the chamber perpendicularly to the molecular beam to eliminate Doppler shift. They ionize a cloud of molecules with a certain spatial distribution. The cloud is accelerated by a two stage system of charged plates to achieve Wiley-McLaren[15] space focusing. This setup consists of a constant voltage lower plate at +2000V and a pulsed voltage upper plate of +3000V. The upper plate is pulsed after the creation of the ions to extract them from the beam and push them towards the detector below. Those ions closer to the pulsed plate but farther from the detector are accelerated more than those farther from the pulsed plate. The ion cloud travels through a voltage free flight zone between the charged plates and the detector. This allows for narrowing of the cloud's spatial distribution as the ions originally farther from the detector catch up with those which started closer.

Once the cloud collides with the detector, the ion's times-of-flight are measured. Since flight time is used to obtain mass measurements, the narrower the ion cloud, the more precisely mass can be measured. This focusing process narrows the flight time distribution of ions of the same mass but does not affect the separation of ions of different masses.

The detector signal is registered on an oscilloscope and is averaged over 8, 16, or 32 laser shots to reduce fluctuations. An example of a snapshot of the oscilloscope output when 9FCA and two of its clusters are being ionized is given in figure 2.2.1.

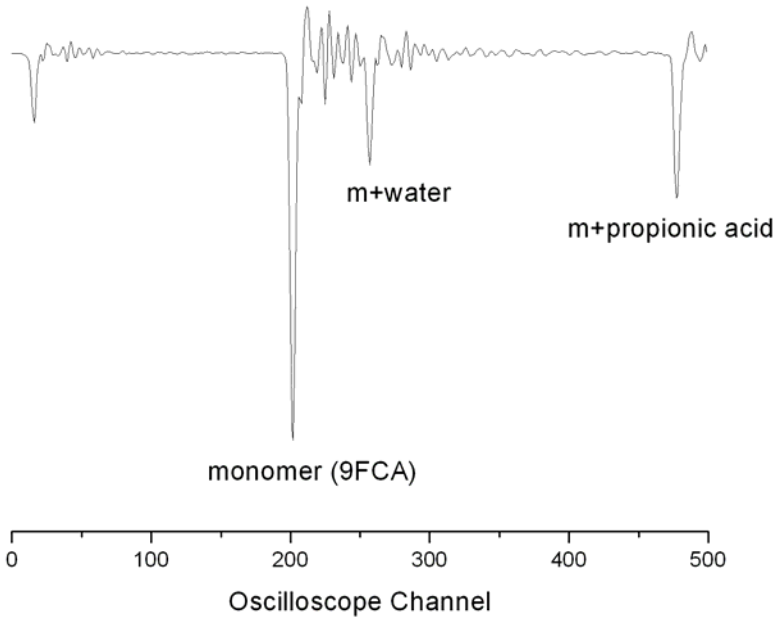

Figure 2.2.1: Sample Oscilloscope Output for TOF Mass Spectrometry

The mass an unknown peak represents can be found by noting that there is a linear relationship between the square root of the molecular mass and the time of flight (or oscilloscope channel, since the two are linearly related). The exact equation relating the masses to times of flight is strongly dependent on experimental conditions such as extraction voltages, laser arrangement and timing, and helium backing

pressure, making it impossible to create a universal fitting curve. Thus, a peak representing a known mass must be present to determine the mass of any unknowns.

2.3: Sample Preparation

The 9FCA sample is prepared by dissolving a small amount of it in acetone and depositing it directly into the nozzle. The acetone is then evaporated and the nozzle attached to the valve inside the chamber. This technique was used previously by Gu to reduce decomposition of the sample[14]. The sample is partially vaporized by heating the nozzle and seeded into the passing helium gas. The exact vapor pressures of the samples are not known; instead, the operating temperatures were determined by finding the maximum signal intensity which showed negligible fragmentation or decomposition products. The various binding partners were prepared by heating in the sample holder. The operating temperature for each was determined by maximizing the 1-1 cluster signal while minimizing clusters with more than one binding partner per chromophore. The 1-1 signal has some dependence on the helium pulse timing and backing pressure as well, so these parameters are optimized simultaneously. It is necessary to minimize higher order cluster concentrations; although they can be mass separated, they tend to fragment and produce hot 1-1 clusters, which unfavorably broaden the spectra.

2.4: Laser Specifications

UV wavelengths were obtained using a pulsed (20 Hz), frequency doubled Nd:YAG laser (Continuum) to pump a tunable dye laser (Lumonics HD500) and doubling the output frequency (Spectra-Physics WEX). IR wavelengths were obtained using a crystal subtraction (Spectra-Physics WEX) of frequency doubled

Nd:YAG (Quanta-Ray GCR-3) pumping a tunable dye laser (Lumonics HD500) output from the non-frequency doubled, infrared, Nd:YAG output.

2.5: Spectroscopic Techniques

REMPI spectra were taken using a one color multiphoton ionization (1+1) approach; the target molecules are excited to the first electronically excited singlet state, S_1, by the first UV photon then ionized by another photon of the same wavelength (figure 2.5.1).

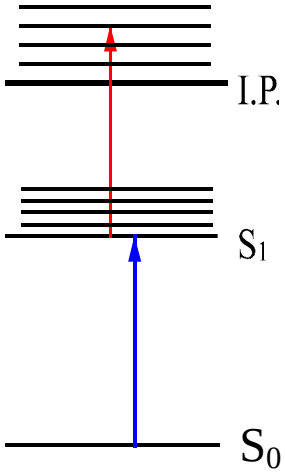

Figure 2.5.1:
REMPI Scheme

Since the same wavelength photon is used for excitation and ionization, the resultant spectra give vibronic information for the S_1 state; photons which don't resonate with a S_0-S_1 transition don't have enough energy to ionize the molecule. Observed S_0-S_1 transitions are typically from the ground state of the molecule to the ground state of the excited state, giving the origin band, or to excited states with excited vibrations. The strongest absorptions are singly excited, single vibrations; weaker multiply excited vibrations, called overtones, and combinations of vibrations, called combination bands, are often observed as well. The origin is typically the most strongly absorbing transition. Hot bands, transitions from a vibrationally excited S_0 state to a vibrationally excited S_1 state, are sometimes observed, especially if the molecule is insufficiently cooled. These generally have lower energies than the origin transition. In one color REMPI, if the S_1 state is separated from the ground state by less energy than it is from the D_0

cation state, then spectra won't be observed. This is rare, however, and the lack of a spectrum usually indicates a rapid relaxation of the S_1 state or another phenomenon.

The IR-UV double resonance technique builds off of REMPI by using a depletion method. The UV laser is tuned to a resonance, usually the origin, of the target molecule. The IR laser is set to scan, timed to fire about 100 ns before the UV. When the IR laser excites a vibration, the ion signal drops because the ionizing UV wavelength is inappropriate for excitation from the vibrational state to the S_1 state and thus ionization (figure 2.5.2).

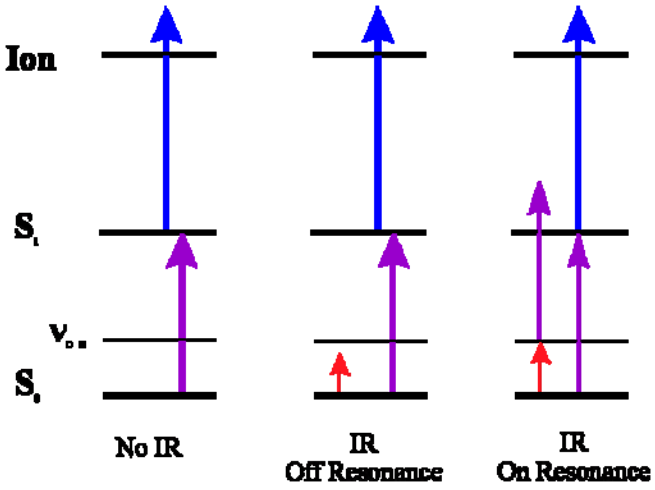

Figure 2.5.2: IR-UV Double Resonance Scheme

This depletion is maximized by spatially overlapping the lasers. This is facilitated by having the IR and UV lasers enter the molecular beam apparatus in a counterpropagating geometry. A depletion percentage of 50% or greater is generally achieved. A shot-to-shot subtraction can be utilized to reduce background noise; the UV laser is pulsed at twice the repetition rate of the IR laser, and the signal with the IR excitation is subtracted from signal without the IR excitation.

The IR-UV hole-burning spectra were obtained through similar principles. The IR laser was tuned to a resonance of the target molecule and the UV spectrum

was scanned. Like in the IR-UV double resonance depletion spectra, the UV signal is depleted by IR resonance. This results after shot-to-shot subtraction in a UV spectrum where only the molecules with the targeted IR resonance appear. Those molecules not depleted by the IR give UV signals with the same strength whether or not the IR is on, so they are removed in the shot-to-shot subtraction. If different conformers have IR resonances which are separated well enough to be excited individually, this should result in a separation of their UV spectra. An example of this process is given in figure 2.4.3.

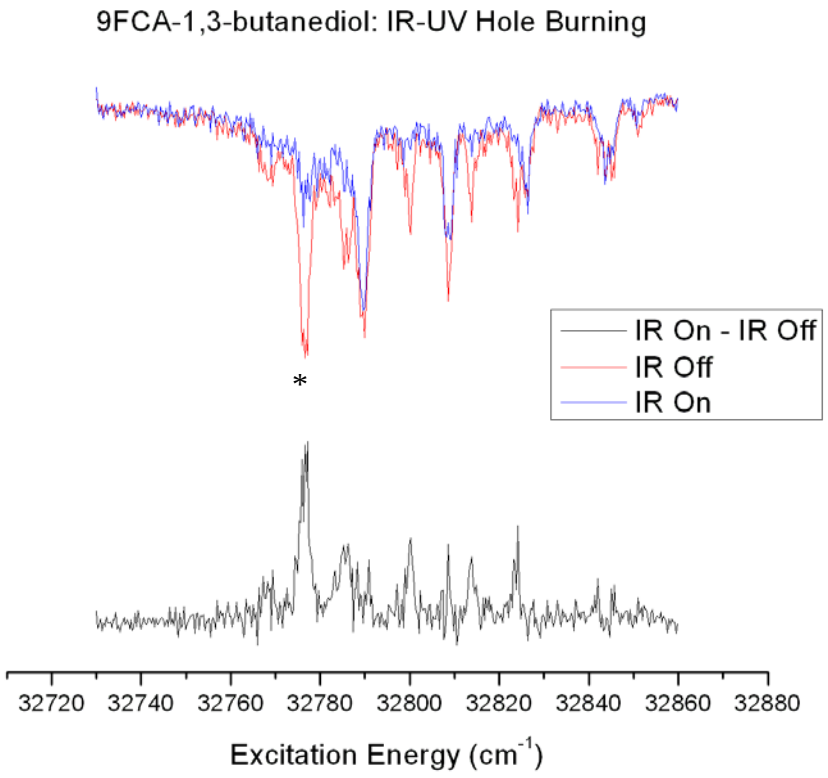

Figure 2.5.3: IR pumping at 3459 cm^{-1}, a vibration belonging to conformer with origin at 32776

2.6: Computational Techniques

The Gaussian 09 program[16] was used for all computational techniques employed including calculation of relative energies, binding energies, and vibrational

frequencies. DFT methods were used in all cases with the B3LYP/6-311++G(d,p) basis set. This was chosen based on previous work in this lab[14], and a study by Lee and Boo[17] which found B3LYP to be quite accurate in predicting the vibrational frequencies and modes of the fluorene molecule. All energies given have taken zero point energy corrections into account. Counterpoise corrected potential energy surfaces were used for calculating binding energies. An empirical linear scaling factor of 0.952 was used for B3LYP calculated vibrational frequencies to correct for systematic error. This was obtained by fitting the experimentally determined 9FCA hydroxyl stretching frequencies with the calculated frequencies. It was found to give better results for 9FCA cluster systems and is within the uncertainty in B3LYP scaling frequencies determined by Johnson et al.[18]

Ch 3: Background

3.1: 9FCA Monomer

Because the work in this thesis is heavily based on prior work by Gu[14], results essential to the understanding of the current work are summarized and useful figures reproduced here. Additional analyses and reevaluations of previous data are given as well.

A computational assay of possible minimum energy structures was performed using the B3LYP/6-311++G(d,p) functional with zero point energy corrections on the 9FCA monomer to see if multiple conformations might be expected to be observed in

the molecular beam. The structures and relative energies of the four lowest energy conformers found are those in figure 3.1.1.

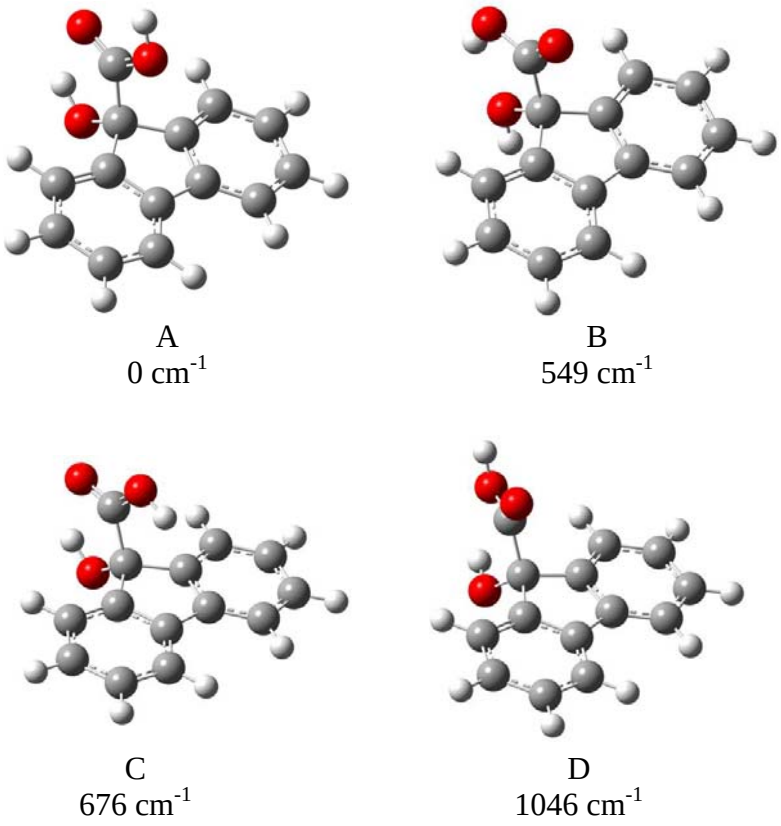

Figure 3.1.1: Lowest Calculated Energy Conformers of 9FCA

The lowest energy structure possesses a C_s symmetry, having its side chain planar and perpendicular to the fluorine ring system. Significant intramolecular bonding between the 9-hydroxy group and the carboxylic acid oxygen is predicted. This conformation is the only one expected to be observable because of the large gap in energy between it and the other calculated conformations. This can be approximately quantified though a Boltzmann population analysis; in a jet cooled spectrum, the relative populations of molecules after cooling are expected to closely reflect the populations prior to expansion if the barriers to isomerization are greater than about 350 cm^{-1}. Even though this equation formally requires knowledge of all the

conformational states of a system, the majority of the conformers have such low populations that they can be omitted. Since the 9FCA system has high enough isomerization barriers between the four calculated conformers, a rough estimate of the percent of molecules in the second lowest energy conformation is found to be 11 percent.

This already low number is most likely an overestimation because conformations not included in the calculation only contribute terms to denominator. Thus, it is not expected to appear in the 9FCA spectrum.

An issue that remains in this analysis is that the populations in the jet do not necessary reflect the observed spectra intensities. These also depend on the absorption characteristics of the molecules. However, for similar systems, such as these 9FCA conformers, this is generally has little differential effect, so the peak intensities observed can be related well to the populations in the molecular beam.

The prediction of only one visible conformer was confirmed by UV-UV hole-burning; the REMPI spectrum and hole-burning spectrum showed no significant differences, indicating that all the spectral features in the REMPI spectrum originate from the conformer with an electronic origin at 32767 cm^{-1} (figure 3.3.2).

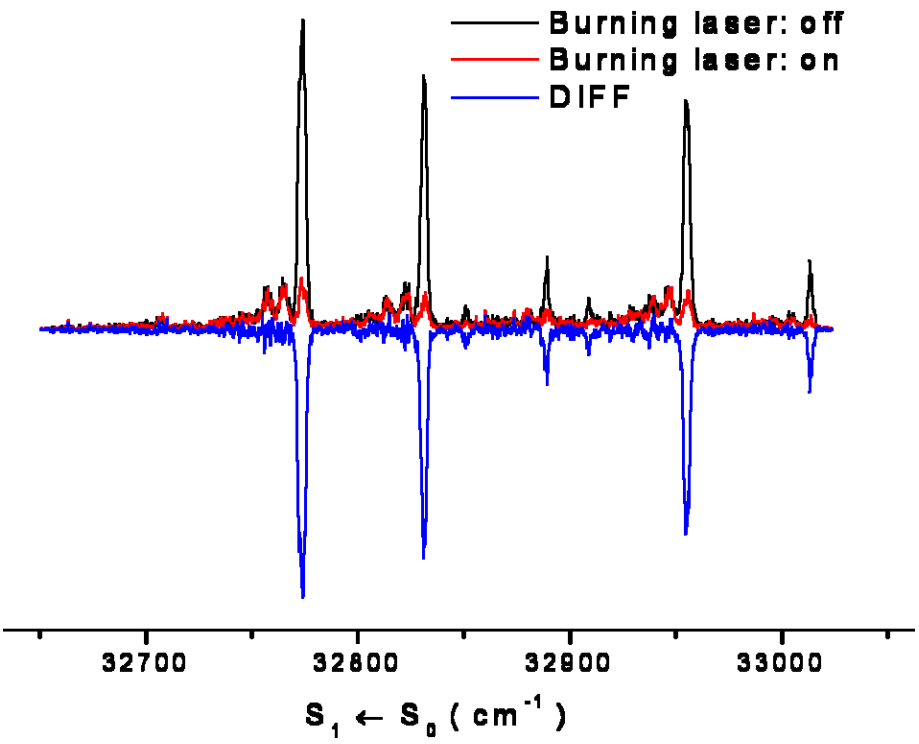

Figure 3.12: Results of UV-UV Hole-Burning of 9FCA Monomer

The vibronic structure of 9FCA was analyzed with regards to excited state calculations and symmetry considerations. The 9FCA ground state symmetry is totally symmetric (A') and the excited state is totally antisymmetric (A"). The molecule was determined to absorb light parallel to the long axis (perpendicular to the mirror plane), an antisymmetric process. Taking the product of the three symmetries (totally symmetric x totally antisymmetric x totally antisymmetric) gives a totally symmetric symmetry. Thus, only totally symmetric vibrations are allowed[19].

The peak at +58 cm^{-1} from the origin was assigned the rocking mode (figure 3.3.3), and the peak at +183 cm^{-1} was assigned the in-plane squeezing mode (figure 3.3.4).

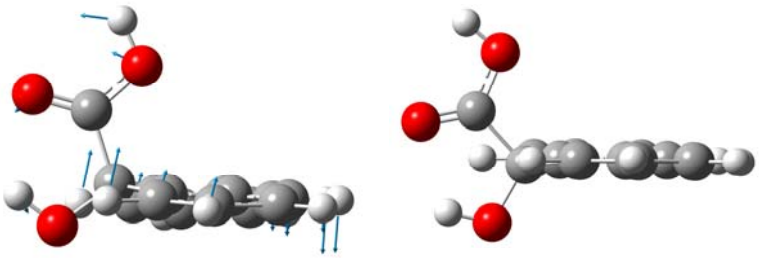

Figure 3.13: 9FCA Rocking Vibration with Frequency = +58 cm^{-1}

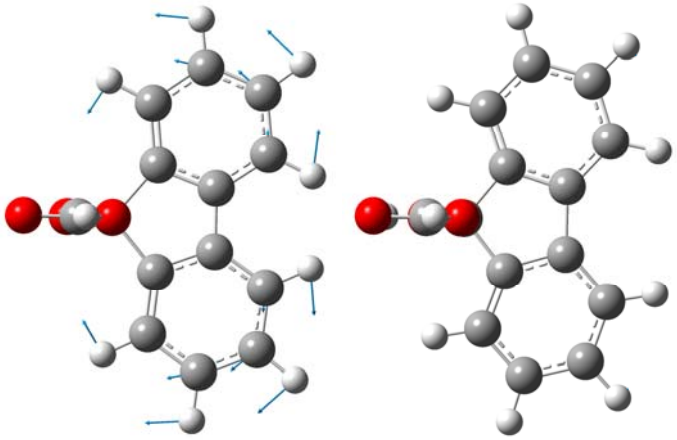

Figure 3.14: 9FCA Squeezing Vibration with Frequency = +183 cm^{-1}

3.2: 9FCA Clusters

Clusters of the 9FCA monomer with the ligands water, benzoic acid, acetic acid, and formamide were also considered. Their REMPI spectra were recorded; the origin of each cluster was aligned to compare the relative shifts and occurrences of their vibronic peaks (figure 3.3.5).

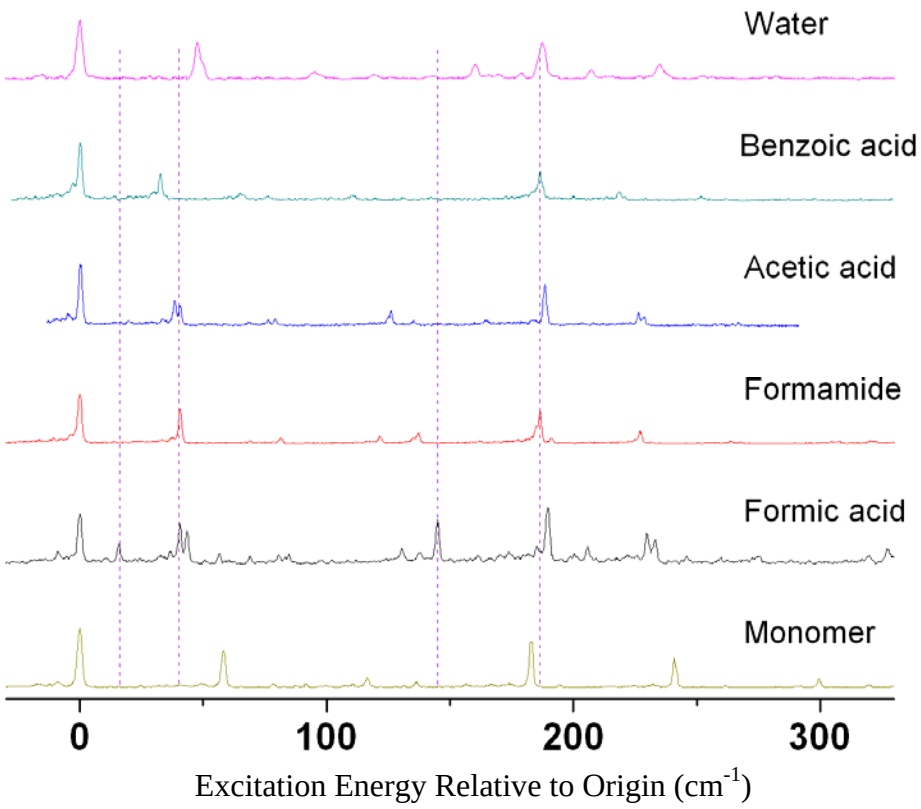

Figure 3.2.1: Comparison of REMPI spectra for 9FCA monomer and various ligands

The spectral features of the clusters are expected to be similar to those of the monomer, with perturbations and activations of additional modes caused by binding induced geometry and electronic changes. One notable trend is the decrease in frequency of the rocking mode of the clusters compared to the 9FCA monomer. For example, the formamide rocking mode is at +40 cm^{-1}, and the corresponding benzoic mode is at +32.7 cm^{-1}. This was explained as the result of increased reduced mass of the side chain–binding partner system compared to the bare side chain of the monomer; more massive objects oscillate at lower frequencies based on a simple harmonic model. Benzoic acid has a larger mass (122.12 g/mol) than formanide (45.04 g/mol), so the rocking mode is frequency is reduced more strongly. The

squeezing mode was only marginally shifted in each cluster; this vibration mostly involves the fluorene ring, so binding is expected to have little effect.

Additional peaks, not present in the monomer, were observed in the formic and acetic acid spectra. This is possibly due to symmetry breaking in the cluster excited state. As discussed, the only the totally symmetric vibrational modes of the monomer are optically active based on its symmetry. The S_1 state of the formic acid was calculated to have a bent side chain (figure 3.3.6), reducing the symmetry of the molecule to C_1.

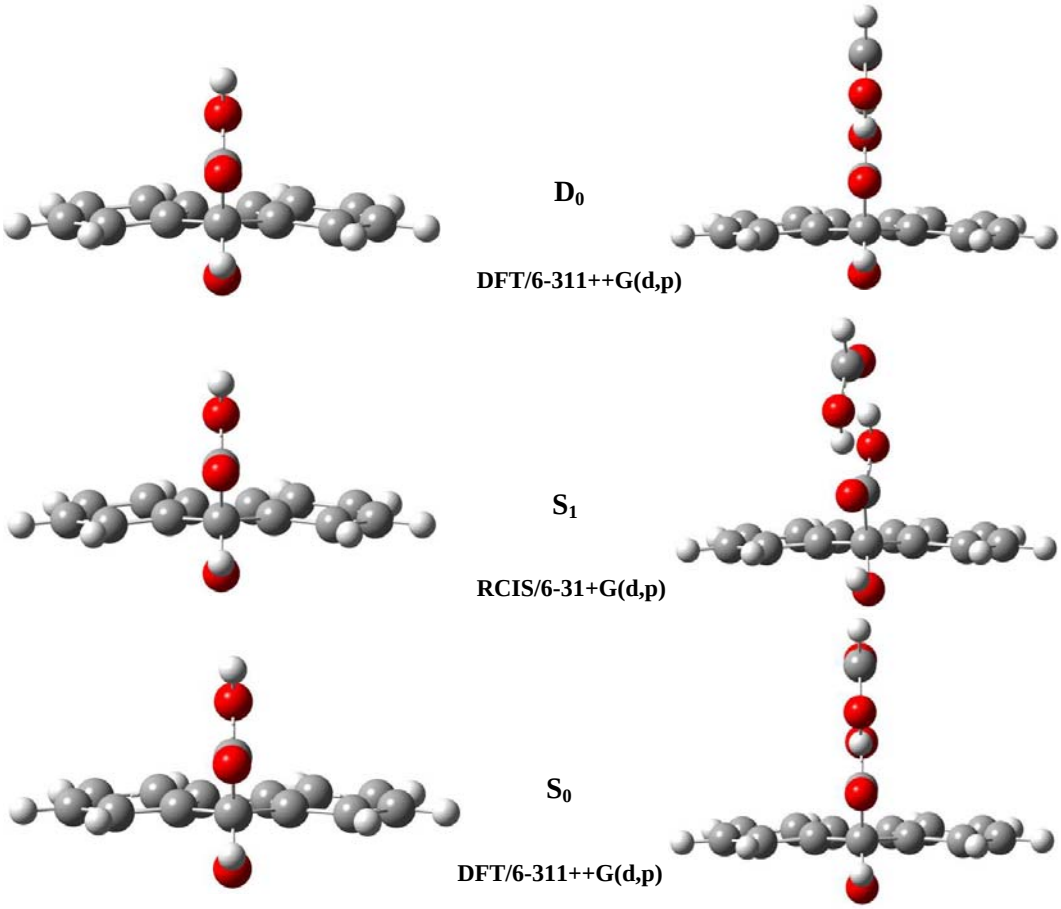

Figure 3.2.2: Comparison of Calculated Structures of 9FCA and 9FCA+Formic Acid

This allows added active vibrations, such as a torsional mode (figure 3.3.7) at +16 cm^{-1}.

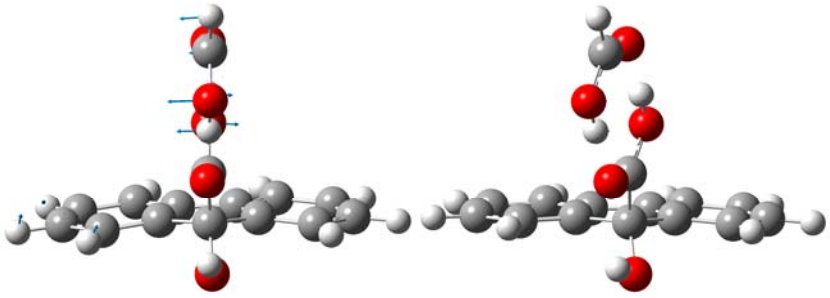

Figure 3.2.3: 9FM-Formic Acid Torsional Vibration with Frequency = +16 cm^{-1}

The band with peaks at +41 and +44 cm^{-1} was assigned to a twisting mode with a splitting of 3 cm^{-1}, with the reasoning that the rocking mode cannot exist in the S_1 state if the 9FCA side chain is bent. However, the peak at +41 cm^{-1} seems to fit nicely with the reduced mass model of the rocking vibration. Furthermore, a band is observed at +85 cm^{-1}, which would be the frequency of a combination band of the +41 and +44 cm^{-1} peaks. Thus, it seems more likely that the rocking mode is still present in the formic acid cluster and the peak at +44 cm^{-1} is an unidentified asymmetric mode.

The acetic acid cluster excited state was expected to be distorted similar to the formic acid cluster; however, excited state calculations were not possible because of limited computational resources.

Ch 4: Results and Discussion

4.1: 9FCA Monomer

9FCA was obtained from Aldrich and used without further purification. It was heated in the nozzle at 120 ^{o}C, and a REMPI spectrum was taken. The origin

transition was found at 32767 cm^{-1} as previously observed; no significant differences existed compared to the previously measured REMPI spectrum.

The IR spectrum was obtained and is shown in figure 4.1.1:

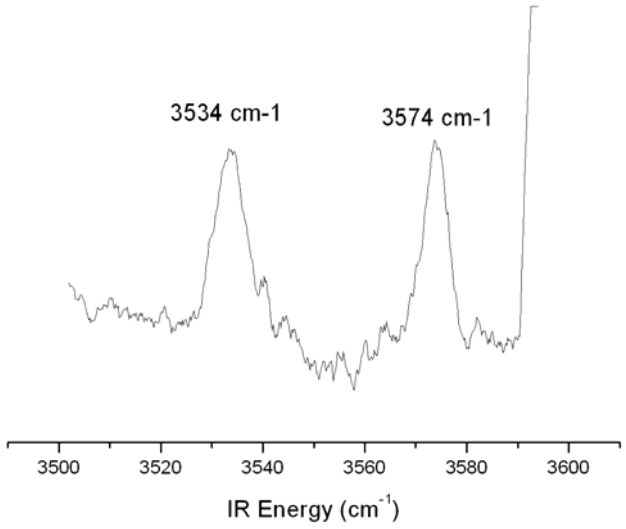

Figure 4.1.1: IR-UV Double Resonance Spectrum of 9FCA, UV Laser Tuned to 32767 cm^{-1}

These peaks were assigned to the OH stretching frequencies of the carboxylic acid (3574 cm^{-1}) and hydroxyl (3534 cm^{-1}) groups, by comparison with the B3LYP calculated frequencies, 3707 $cm^{-1}$and 3664 cm^{-1}. This gave an average percent difference of 3.577. The near-vertical line at the blue end of the spectrum occurred when the UV laser was blocked. This gives a reference for the percent depletion obtained; here it is at about 60 percent.

4.2: 9FCA-Acrylic Acid

Acrylic acid was chosen as a binding partner for 9FCA because of its conformational flexibility and similarity to carboxylic acid systems previously studied. Two conformers were predicted to be observable based on relative energies: a “cis” conformation with the acid carbon chain of the acid on the same side as the

fluorene ring and a “trans” conformation with them in opposite orientations (figure 4.2.1).

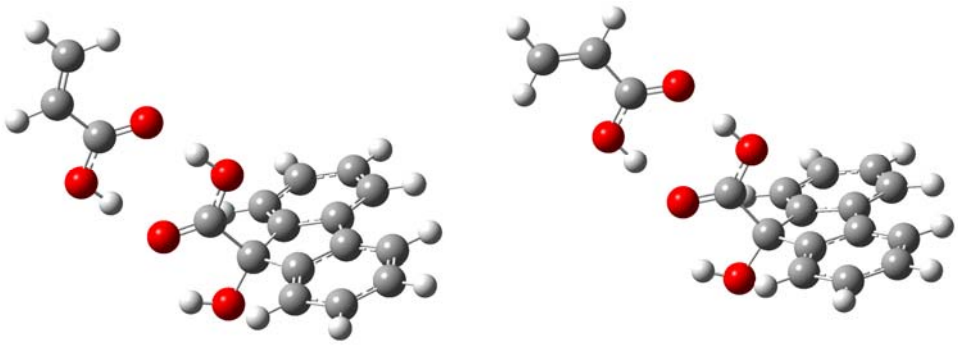

Cis
0 cm-1

Trans
11 cm-1

Figure 4.2.1: Two Lowest Energy Conformers of 9FCA-Acrylic Acid (calculated)

UV-UV hole-burning was performed to test this theory, with the burn laser tuned to the origin at 32765 cm^{-1}. Figure 4.2.2 displays the results with the standard REMPI spectrum on top and the result of the hole-burning on bottom.

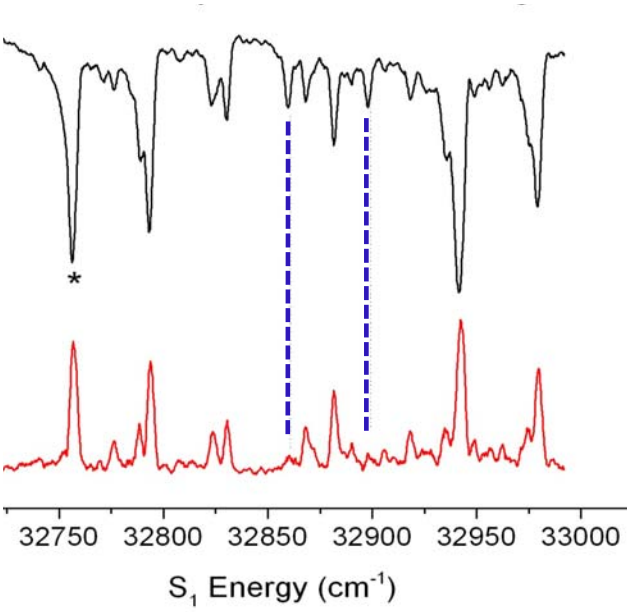

Figure 4.2.2: UV-UV Hole-Burning Spectrum of 9FCA-Acrylic Acid

Surprisingly, two small, largely blue shifted peaks were the only ones visibly subtracted. However, these subtracted peaks have nearly the same difference between them as do the main origin and that conformer's next large resonance. Thus, these removed peaks might represent a second conformation with a similar geometry as the dominant one.

The dominant conformer spectrum follows a similar peak progression to formic acid cluster. A torsional mode is observed at +18 cm^{-1}, implicating a similar symmetry breaking in the excited state. A rocking mode is seen at 36 cm^{-1}, a lower energy than the 40 cm^{-1} rocking mode of the less massive formic acid, as expected. This seems to support that the acrylic acid has the same type of hydrogen bonding interaction as formic acid, so the calculated conformers should be the lowest energy ones.

Therefore, it is predicted that the two subtracted peaks belong to one of the calculated conformers, and that this conformer is not strongly spectrally activated, although it is difficult to tell why. The large blue shift of the origin of the second conformer might indicate a large decrease in the binding energy of the excited state compared to the ground state; however, more complicated electronic effects could certainly cause this as well.

Attempts were made at performing the same type of analysis with clusters formed with propionic and pyruvic acid to see if they demonstrated similar behavior; each had a calculated low energy second conformer. However, neither cluster gave usable REMPI spectra. In particular, the pyruvic acid cluster measurements were plagued by contamination from dissociation of higher order clusters.

4.3: 9FCA-(1,3-Propanediol)

9FCA was complexed with 1,3-propanediol by heating the diol to 120 ^{o}C in the sample chamber. The 1-1 clusters and monomer were mass selected and the REMPI spectrum taken (figure 4.3.1).

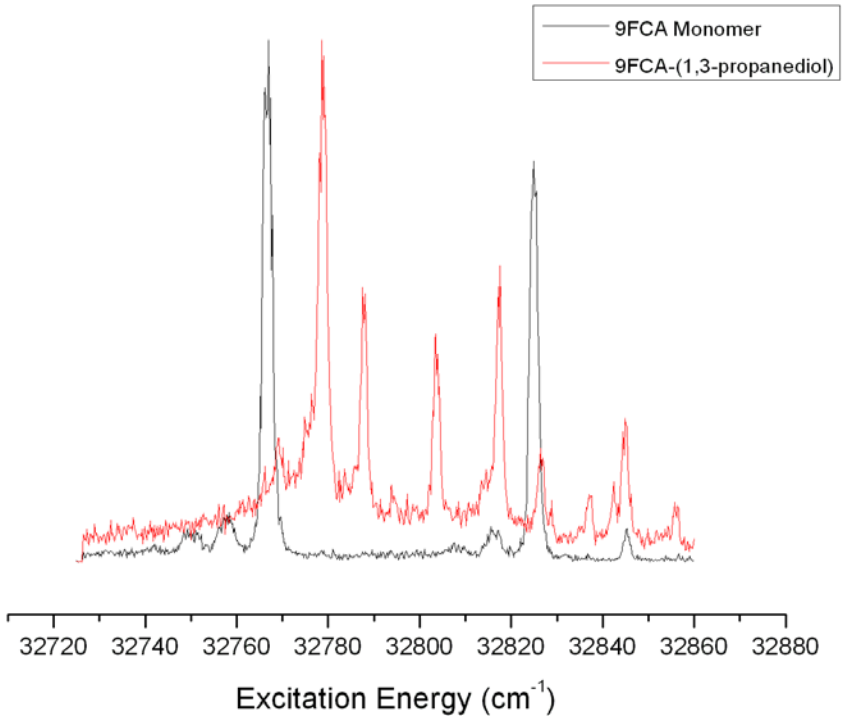

Figure 4.3.1: REMPI Spectra of 9FCA Monomer and 9FCA-(1,3-propanediol)

The cluster spectrum indicates several vibrational modes not detected in the 9FCA monomer. Although the 9FCA-(1,3-propanediol) system has no symmetry in the ground state, unlike the earlier described carboxylic acid systems studied by Gu, its spectral features can be analyzed similarly. This is because it is symmetric other than the asymmetry in the diol orientation.

While the same selection rules governing the appearance of vibronic bands do not formally apply to the cluster, in practice they are generally observed for systems

with small perturbations such as this one. Therefore, the band at +39 cm^{-1} is tentatively assigned the rocking vibration, analogous to the carboxylic acid cluster vibrations. This nicely fits with the previous correlation of binding partner mass and frequency. 1,3-propanediol (76.09 g/mol) weighs less than benzoic acid and more than formamide, and its rocking vibration is intermediate to the two as well. The other peaks are less straightforward to assign. An excited state frequency calculation could be used help to identify them, but it is unfortunately unfeasible with our current computational resources. The band at +9 cm^{-1} is likely a torsional mode because of its low frequency. The bands at +25 cm^{-1} and +66 cm^{-1} are difficult to assign but might represent intermolecular modes or the twisting motion of the 9FCA side chain. The other smaller peaks probably indicate overtone and combination bands. Table 4.3.1 contains the assignments made.

Band Energy (cm-1)	Vibrations Excited
9	Torsion
25	?
39	Bend
48	9+39
50	2*25
59	2*25+9
64	25+39
66	?
78	2*39

Table 4.3.1: Tentative Assignment of 9FCA-(1,3-Propanediol) Vibrations

Figure 4.3.2 shows the IR spectrum. Three peaks were observed in the scanned region.

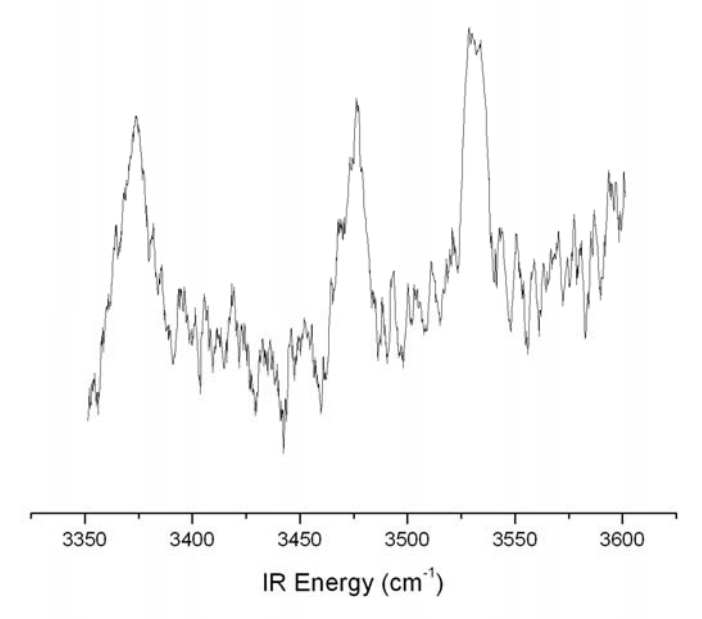

Figure 4.3.2: IR Spectrum of 9FCA-(1,3-Propanediol) Cluster

To assign these peaks to specific vibrations, as well as to find the correct bonding geometry with which to assign them, computational results were compared to the experimental results. Three feasible structures were found, which will be referred to as looping, bridging, and straight (figure 4.3.3).

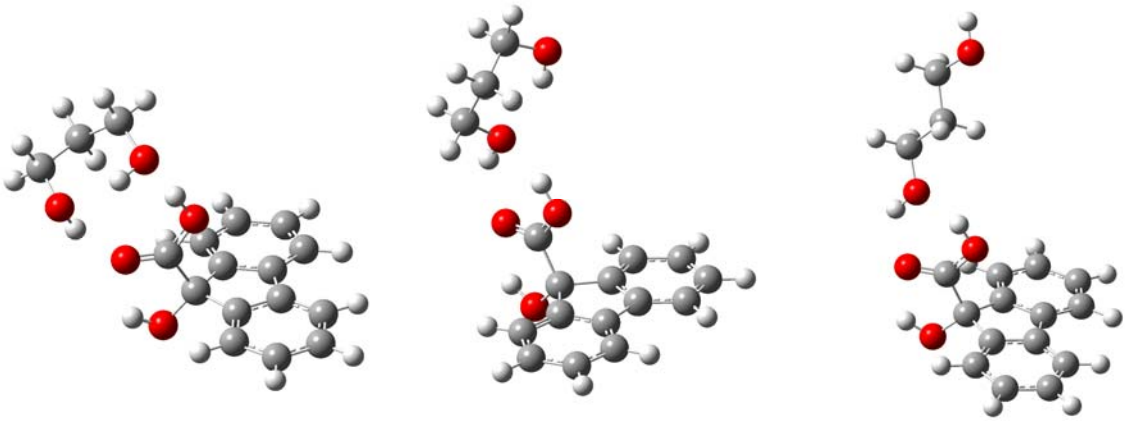

Looping
0 cm^{-1}

Bridging
1438 cm^{-1}

Straight
1985 cm^{-1}

Figure 4.3.3: Lowest Energy Calculated Conformations of 9FCA-(1,3-Propanediol) Cluster

The looping conformation is the one conjectured to be what was observed experimentally because it has the lowest calculated energy by a large margin. A Boltzmann population analysis indicates that lower than 0.5 percent of the bridging conformer is present in the beam and even less of the straight conformer.

However, since the computational methods used only find local minima near an input geometry, it is of course possible this prediction is wrong. To attempt to add weight to this prediction, OH vibrational frequencies were calculated for the ring and bridging structures and compared to the observed frequencies (figure 4.3.4).

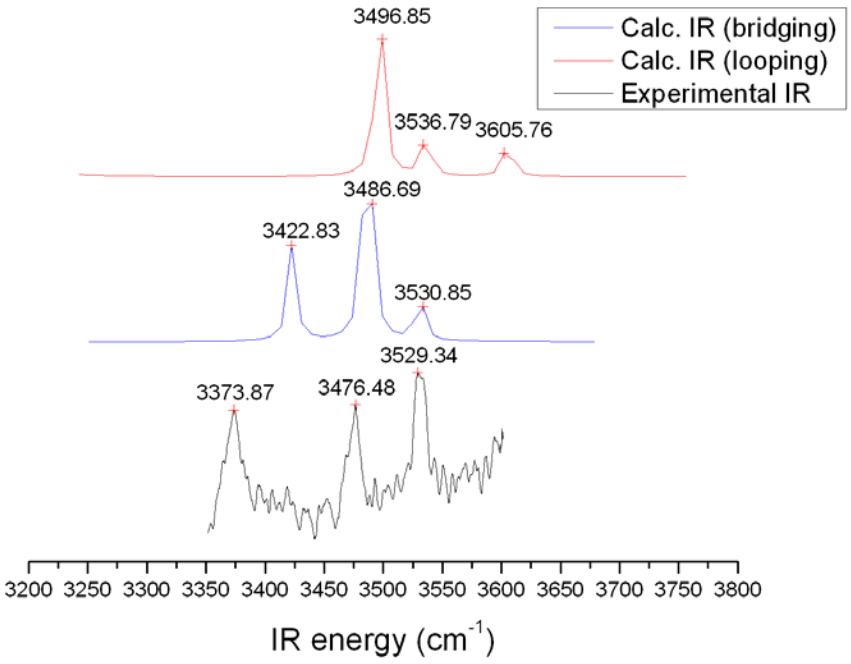

Figure 4.3.4: Comparison of 9FCA-(1,3-Propanediol) Calculated IR Frequencies with Observed Frequencies

The looping structure vibrations better agree with the experimental values, giving an average percent error of 0.65% compared with the error for the bridging structure of 2.1% and the straight structure of 3.4%. Assuming the looping structure to be correct, the IR bands can be assigned as in figure 4.3.5.

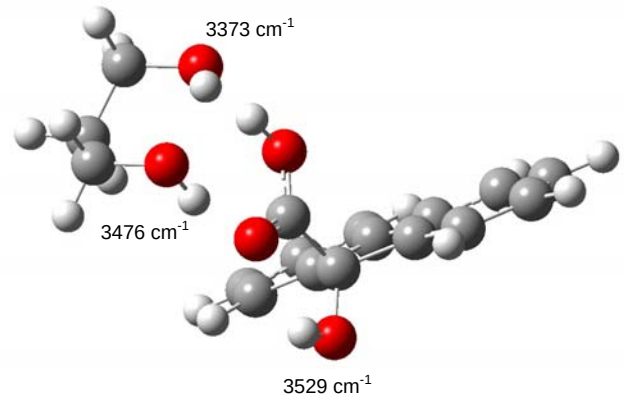

Figure 4.3.5: Assignment of observed IR bands to OH Stretches

The fourth hydroxyl stretching frequency in both calculated geometries was predicted to lie far outside of the spectral region scanned. Attempts to find this other IR signal have failed; although, no signal was seen at all in those attempts, even when using a known reference, indicating a problem with the experimental setup at the time.

4.4: 9FCA-(1,3-Butanediol)

The cluster was prepared by heating 1,3-butanediol in the sample chamber at 115 ^{o}C. The obtained REMPI spectrum is shown in figure 4.4.1.

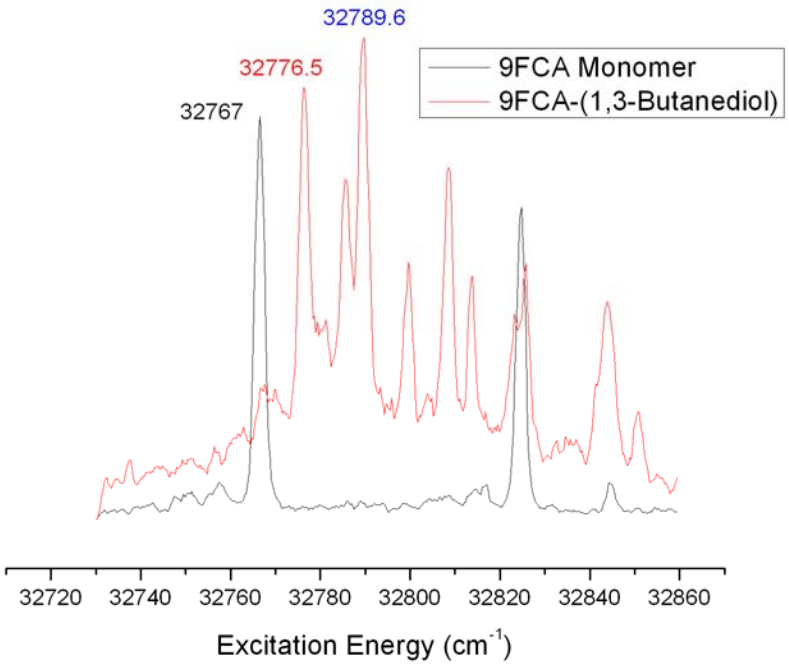

Figure 4.4.1: REMPI Spectra of 9FCA Monomer and 9-FCA-(1,3-Butanediol)

Despite the similarity in structure between 1,3-butanediol and 1,3-propanediol, this spectrum is much more complicated than that of the 1,3-propanediol cluster. A possible explanation for this would be the significant concentration of more than one conformer in the molecular beam. IR spectra were taken depleting the with UV tuned to two strongest peaks in the REMPI spectra, 32776 cm^{-1} and 32789 cm^{-1}, those being the most likely to be the strongly absorbing origins (figure 4.4.2).

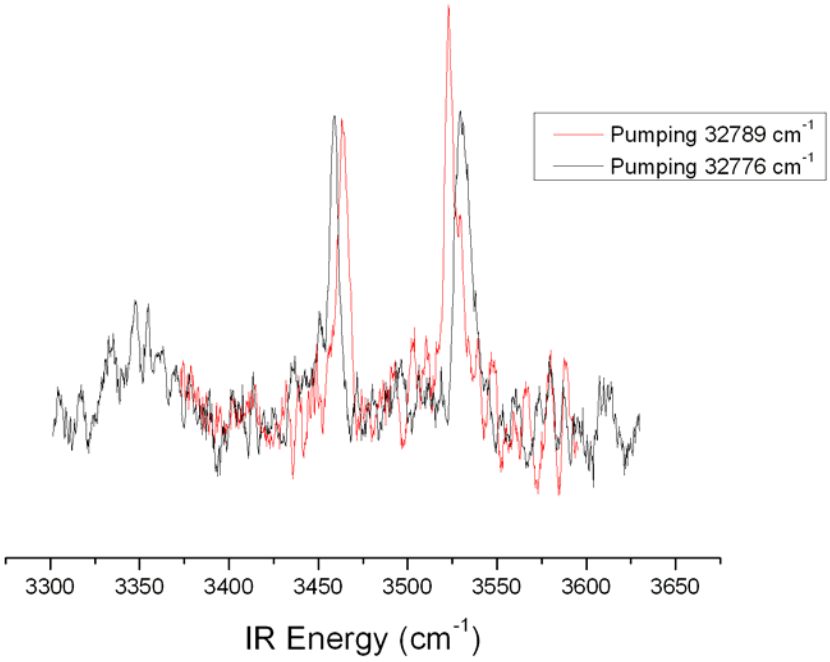

Figure 4.4.2: IR spectra of 9-FCA-(1,3-Butanediol), Pumping 32789 cm^{-1} and 32776 cm^{-1}

Two distinguishable sets of peaks were observed. To make sure that they denoted different conformers and were not instead produced by experimental error, as well as to hopefully simplify the REMPI spectrum, IR-UV hole-burning was used, pumping one of each set of IR resonances. Figure 4.4.3, the overlaid results, confirms that two major conformations are present. Each seems to have a similar peak arrangement as 1,3-propanediol. Combined with the similarity of the molecular structures, this seems to indicate that both bond with similar geometries.

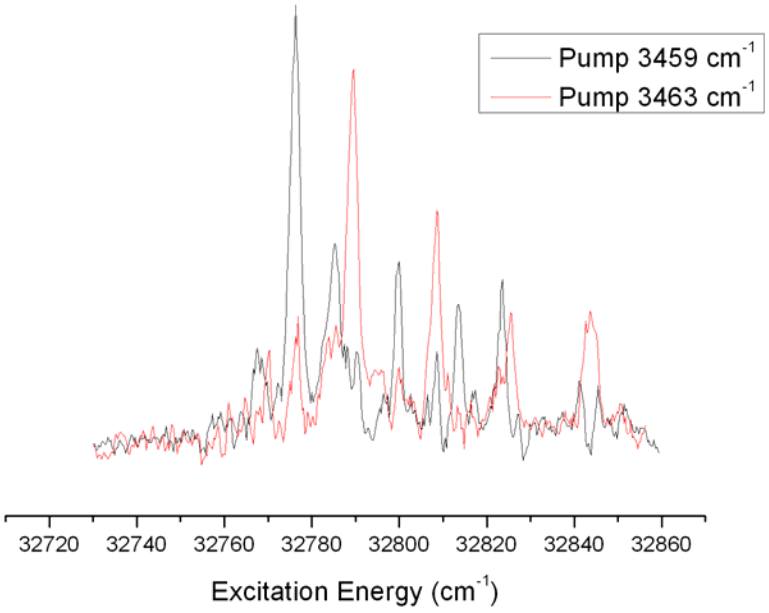

Figure 4.4.3: Overlay of IR-UV Hole-Burning Spectra, Pumping IR at 3459 cm^{-1} and 3463 cm^{-1}

The four lowest energy conformations are predicted to be those in figure 4.4.4, based on the established geometry of the complex with 1,3-propanediol.

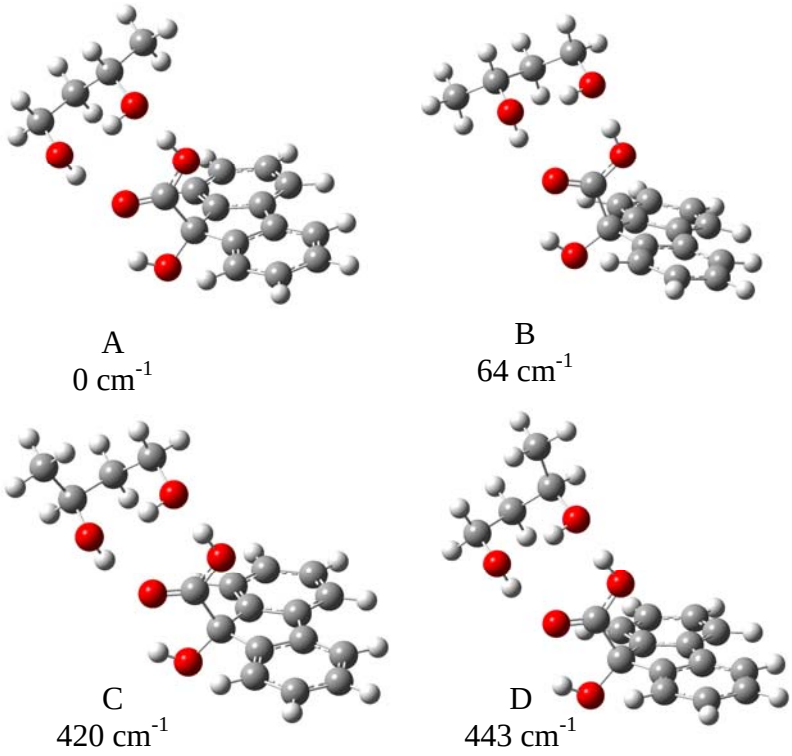

Figure 4.4.4: Lowest Energy Calculated Conformations of 9FCA-(1,3-Butanediol)

These differ only by conformations of the diols, causing the carbon chain to be oriented differently in each, since they all have the same binding geometry. The lowest energy conformation is tentatively assigned the origin at 32789.6 cm^{-1}; similar studies have suggested that the strongest origin transition indicates the lowest energy conformation[20, 21]. A comparison of the calculated IR spectrum with the experimental one (table 4.4.1) was performed to attempt to substantiate this claim; however, the results were inconclusive because the differences in experimental peak frequencies between the conformers are too small to discriminated by theoretical calculation.

Conformer	Calc Freq. 1	Observed Freq.	difference	Calc Freq. 2	Observed Freq.	diff	Ave. % Error
A	3481	3463	18	3531	3523	7	0.240
B	3477	3459	18	3531	3530	1	0.186
A	3481	3459	22	3531	3530	1	0.217
B	3477	3463	14	3531	3523	8	0.210

Table 4.4.1: Differences Between Calculated and Experimental IR Frequencies (cm^{-1}) For Assignment of Both IR Spectra to Both Conformers

It is possible this analysis could be strengthened by improvement of the experimental results. The IR spectra show only two peaks per conformer; three are expected, like in the 1,3-propanediol system. It is likely this discrepancy is due to experimental error. There is a hint of a peak at the red end of one spectrum and the other was not scanned as far. Retaking the IR spectra in this region would perhaps lead to the detection of the missing peak, which would add another data point to the analysis. It is probable that these peaks are similarly not separated well enough for a comparison with calculated data to yield useful results, though. The fourth peak OH stretching peak, like in the 1,3-propanediol cluster, is expected to fall far to the red in a region which we failed to see signal in. According to the calculations, this vibration

is more sensitive to the difference in conformers. If this is true in the experimental results as well, it may serve as a better diagnostic peak for assigning conformations.

Despite these problems, the vibrational data for the calculated vibrational frequencies provide close matches to the observed experimental IR peaks, indicating that the binding geometry is probably correct even if absolute identification of conformers is not possible through this method.

A Boltzmann population analysis was performed indicating that the one might expect, if significant isomerization does not occur during cooling, 45 percent conformer A, 35 percent conformer B, and 10 percent conformers C and D in the beam. Since two conformers were seen in the S_0-S_1 spectrum, the results of population analysis can be compared to the origin peak heights to get an idea of how well the analysis approximates the spectrally observed conformer ratio. The ratio of origin peak heights is 1:1.11, and the ratio of conformers in the population analysis was found to be 1:1.28. This seems to be quite good agreement, suggesting that the electronic properties are similar for both molecules and that cooling in the beam did not create distributions far from the Boltzmann distributions in this case.

4.5: 9FCA-(1,2-propanediol)

The 1,2-propanediol sample was prepared by heating it to 90 ^{o}C in the sample chamber. The REMPI spectrum is presented in figure 4.5.1.

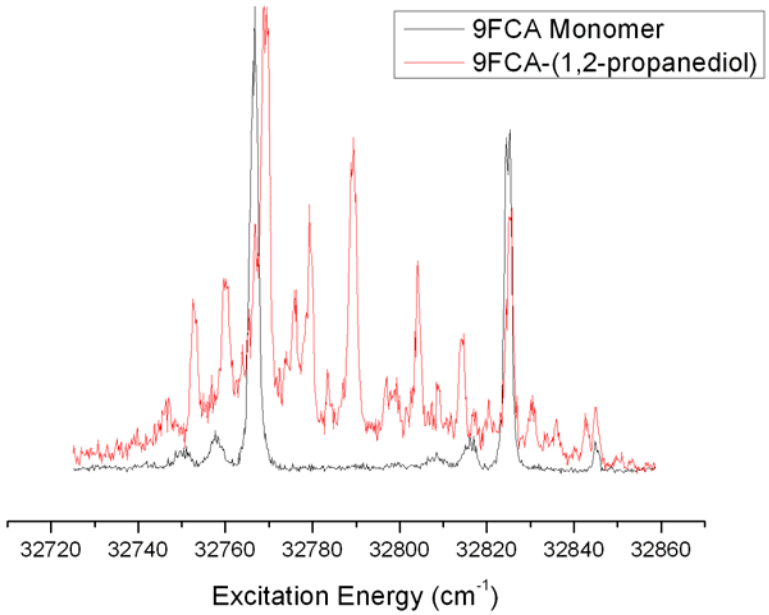

Figure 4.5.1: REMPI Spectra of 9FCA Monomer and 9-FCA-(1,2-Propanediol)

The complexity of the spectrum again suggests the possibility of multiple conformations. Indeed, the computational results (figure 4.5.2) support this supposition.

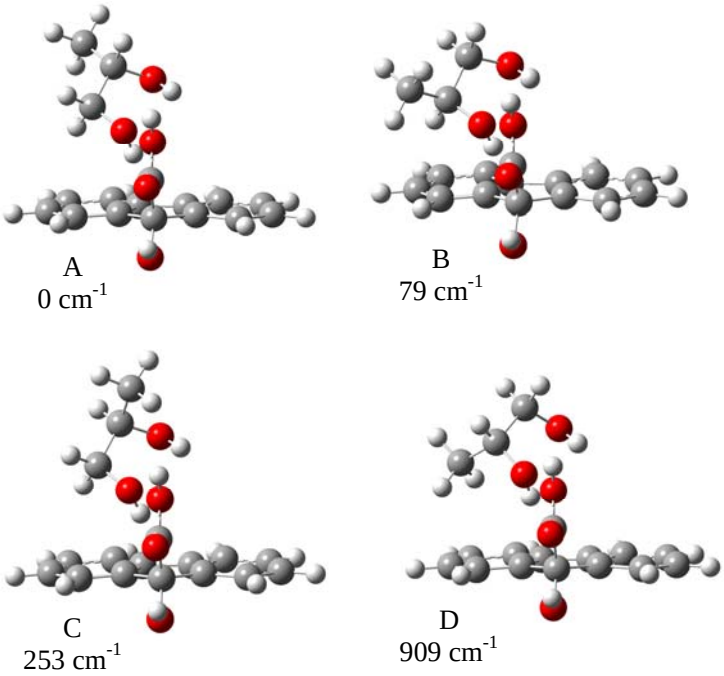

Figure 4.5.2: Lowest Energy Calculated Conformations of 9FCA-(1,2-propanediol)

A Boltzmann population analysis predicts a distribution of 46 percent conformer A, 34 percent conformer B, 18 percent conformer C, and 1.6 percent conformer D. Therefore, conformers A and B are expected to dominate the spectroscopies performed.

To attempt to resolve the different conformer signals, IR spectra were taken by depletion of the REMPI peaks at 32769 cm^{-1} (figure 4.5.3) and 32789 cm^{-1}; however, they were indistinguishable. An IR-UV hole-burning spectrum therefore could not be obtained as it was with the 1,3-butanediol system. UV-UV hole-burning was attempted as well, but it has proven difficult because of the lack of strong, clean UV signal.

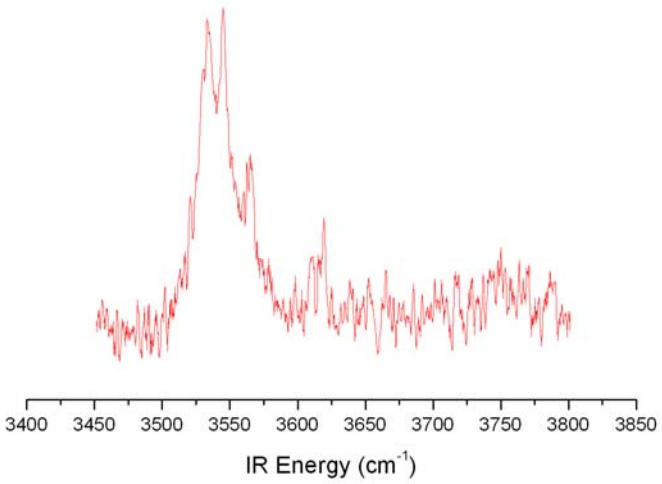

Figure 4.5.3: IR spectra of 9-FCA-(1,2-Propanediol), Pumping 32769 cm^{-1}

Nonetheless, the IR spectrum presents some interesting information on the complex. Significant differences from those obtained for the 1,3-OH complexes are observed. 1,2-propanediol has its hydroxyl groups one carbon closer together. This creates a less favorable bonding geometry; the diol hydroxyl corresponding to that which forms an intermolecular hydrogen bond in the 1,3-OH complexes is instead skewed

outward. This is reflected in a comparison of the binding energies of the complexes of 1,3-propanediol and 1,2-propanediol; they are 4549 cm^{-1} and 3962 cm^{-1}, respectively.

Also, there is significant mixing of the calculated vibrations at 3526 cm^{-1} and 3534 cm^{-1} (figure 4.5.4); if this model is right it would explain why the observed IR absorbance is so broad.

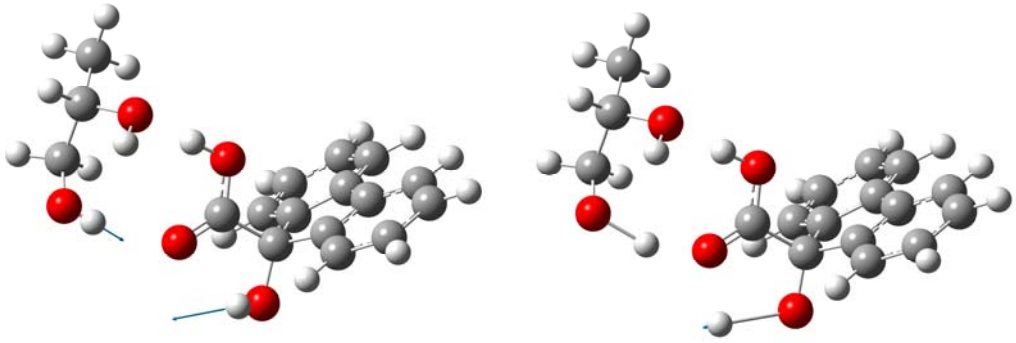

Figure 4.5.4: Calculated Vibrational Mode at 3534 cm^{-1} Strongly Mixing with Mode at 3526 cm^{-1}

Ch 5: Conclusion

The spectroscopic and computational techniques discussed here form a powerful toolset for inquiring into detailed molecular and molecular cluster parameters. They were applied to hydrogen bound clusters of 9FCA with varying levels of success. The 1,3-propanediol cluster seemed to give clear results which could be used further for the deeper analysis of a basic diol, carboxylic acid interaction. The 9FCA-(1,3-butanediol) system in particular showed interesting conformational behavior, which may also exist in the cluster with 1,2-propanediol. However, it is not certain. Perhaps a good way to approach this problem would be to obtain spectroscopic data on the cluster with 1,2-ethanediol, which could serve as a

simpler analogue in the way that the 1,3-propanediol cluster did. The acrylic acid cluster presents intriguing questions centered on the possibility of a second conformer with interesting electronic properties. If the conformer actually exists and can be better characterized, it would certainly be of use in exploring a wider range of cluster behavior. Our lab has previously observed several clusters of 9FCA which for an unknown reason produce no REMPI spectra. If this conformation with a nearly nonexistent spectrum has similar characteristics to those clusters, it would be of great use in explaining the underlying phenomenon.

Ch 6: References

1. Kantrowitz, A.; Grey, J., A High Intensity Source for the Molecular Beam .1. Theoretical. *Review of Scientific Instruments* **1951,** 22, (5), 328-332.
2. Smalley, R. E.; Wharton, L.; Levy, D. H., Molecular Optical Spectroscopy with Supersonic Beams and Jets. *Accounts of Chemical Research* **1977,** 10, (4), 139-145.
3. Levy, D. H., Laser Spectroscopy of Cold Gas-Phase Molecules. *Annual Review of Physical Chemistry* **1980,** 31, 197-225.
4. Pratt, D. W., High resolution spectroscopy in the gas phase: Even large molecules have well-defined shapes. *Annual Review of Physical Chemistry* **1998,** 49, 485.
5. Dessent, C. E. H.; Muller-Dethlefs, K., Hydrogen-bonding and van der Waals complexes studied by ZEKE and REMPI spectroscopy. *Chemical Reviews* **2000,** 100, (11), 3999-4021.
6. Mcclain, W. M., 2-Photon Molecular Spectroscopy. *Accounts of Chemical Research* **1974,** 7, (5), 129-135.
7. Lee, S. J.; Min, A.; Kim, Y.; Ahn, A.; Chang, J.; Lee, S. H.; Choi, M. Y.; Kim, S. K., Conformationally resolved structures of jet-cooled acetaminophen by UV-UV hole-burning spectroscopy. *Physical Chemistry Chemical Physics* **2011,** 13, (37), 16537-16541.
8. Guchhait, N.; Ebata, T.; Mikami, N., Structures of hydrogen-bonded clusters of benzyl alcohol with water investigated by infrared-ultraviolet double resonance spectroscopy in supersonic jet. *Journal of Chemical Physics* **1999,** 111, (18), 8438-8447.
9. He, Y. G.; Wu, C. Y.; Kong, W., A theoretical and experimental study of water complexes of m-aminobenzoic acid MABA center dot(H2O)(n) (n = 1 and 2). *Journal of Physical Chemistry A* **2005,** 109, (5), 748-753.
10. Gerhards, M.; Perl, W.; Kleinermanns, K., Rotamers and Vibrations of Resorcinol Obtained by Spectral Hole-Burning. *Chemical Physics Letters* **1995,** 240, (5-6), 506-512.
11. Scherzer, W.; Selzle, H. L.; Schlag, E. W., Identification of Spectra of Mixed Structural Isomers Via Mass Selective Hole-Burning in the Gas-Phase. *Chemical Physics Letters* **1992,** 195, (1), 11-15.
12. Mitsuzuka, A.; Fujii, A.; Ebata, T.; Mikami, N., Infrared spectroscopy of OH stretching vibrations of hydrogen-bonded tropolone-(H2O)(n) (n=1-3) and tropolone-(CH3OH)(n) (n=1 and 2) clusters. *Journal of Chemical Physics* **1996,** 105, (7), 2618-2627.
13. Dunbar, R. C.; Hopkinson, A. C.; Oomens, J.; Siu, C. K.; Siu, K. W. M.; Steill, J. D.; Verkerk, U. H.; Zhao, J. F., Conformation Switching in Gas-Phase Complexes of Histidine with Alkaline Earth Ions. *Journal of Physical Chemistry B* **2009,** 113, (30), 10403-10408.
14. Gu, Q. L. Spectroscopy and Dynamics of Molecular Clusters: van der Waals Complexes to Hydrogen Bonded Systems. Wesleyan University, Middletown, CT, 2009.

15. Wiley, W. C.; McLaren, I. H., Time-of-Flight Mass Spectrometer with Improved Resolution. *Review of Scientific Instruments* **1955,** 26, (12), 1150-1157.
16. Gaussian 09, Revision A.1, Frisch, M. J.; Trucks, G. W.; Schlegel, H. B.; Scuseria, G. E.; Robb, M. A.; Cheeseman, J. R.; Scalmani, G.; Barone, V.; Mennucci, B.; Petersson, G. A.; Nakatsuji, H.; Caricato, M.; Li, X.; Hratchian, H. P.; Izmaylov, A. F.; Bloino, J.; Zheng, G.; Sonnenberg, J. L.; Hada, M.; Ehara, M.; Toyota, K.; Fukuda, R.; Hasegawa, J.; Ishida, M.; Nakajima, T.; Honda, Y.; Kitao, O.; Nakai, H.; Vreven, T.; Montgomery, Jr., J. A.; Peralta, J. E.; Ogliaro, F.; Bearpark, M.; Heyd, J. J.; Brothers, E.; Kudin, K. N.; Staroverov, V. N.; Kobayashi, R.; Normand, J.; Raghavachari, K.; Rendell, A.; Burant, J. C.; Iyengar, S. S.; Tomasi, J.; Cossi, M.; Rega, N.; Millam, N. J.; Klene, M.; Knox, J. E.; Cross, J. B.; Bakken, V.; Adamo, C.; Jaramillo, J.; Gomperts, R.; Stratmann, R. E.; Yazyev, O.; Austin, A. J.; Cammi, R.; Pomelli, C.; Ochterski, J. W.; Martin, R. L.; Morokuma, K.; Zakrzewski, V. G.; Voth, G. A.; Salvador, P.; Dannenberg, J. J.; Dapprich, S.; Daniels, A. D.; Farkas, Ö.; Foresman, J. B.; Ortiz, J. V.; Cioslowski, J.; Fox, D. J. Gaussian, Inc., Wallingford CT, 2009. In.
17. Lee, S. Y.; Boo, B. H., Density functional theory study of vibrational spectra of fluorene. *Journal of Physical Chemistry* **1996,** 100, (21), 8782-8785.
18. Irikura, K. K.; Johnson, R. D.; Kacker, R. N., Uncertainties in scaling factors for ab initio vibrational frequencies. *Journal of Physical Chemistry A* **2005,** 109, (37), 8430-8437.
19. Gu, Q. L. K., J.L., Binding energy measurement of a carboxylic acid water dimer using infrared-ultraviolet double resonance spectroscopy. **2012,** Manuscript submitted for publication.
20. Basu, S.; Knee, J. L., Conformational studies of the neutral and cation of several substituted fluorenes. *Journal of Electron Spectroscopy and Related Phenomena* **2000,** 112, (1-3), 209-219.
21. Basu, S.; Knee, J. L., Conformational analysis and dynamics of 9-propylfluorene and 9-ethylfluorene. *Journal of Physical Chemistry A* **2001,** 105, (24), 5842-5848.